International Conference on Mechanical, Industrial and Materials Engineering 2017 (ICMIME2017)
28-30 December, 2017, RUET, Rajshahi, Bangladesh.

Paper ID: FM-244

A Numerical Study on the Fluid Structure Interaction of a Wind Turbine Blade

Sumaiya Tasnim*, Md. M. Islam, Shabnoor M. Joty, Zahir U. Ahmed

[1]Department of Mechanical Engineering, Khulna University of Engineering & Technology, Khulna-9203, Bangladesh.
**E-mail: sumaiyatasnim114@gmail.com*

Abstract

Alternative energy is rapidly gaining importance due to the shortage of fossil fuels. As wind energy is one of the most promising forms, wind turbine has become the focus of energy based research to harness this wind energy more effectively. Although many research had previously been conducted for both flow behaviors and structural robustness of wind turbine blade, but mostly for relatively high twist angles (>20º). As such, in this paper a numerical study is performed for a low twist angle in order to investigate fluid flows around a typical horizontal axis wind turbine (HAWT) blade and 1-way fluid structure interaction (FSI). A 9.5 meter long blade has been designed and simulated via ANSYS v16.0 using SST k-ω turbulence model. The structural robustness due to the effect of this load was performed by ANSYS Static Structure. The effect of different free stream wind velocities ranging 4m/s to 12m/s on the flow field and fluid-solid interaction is studied. The flow recirculation occurs near the blade root, and its intensity increases with free stream velocity. Although deflections are mainly observed near the tip, but critical stress developed near the root. Finally, a linear power curve against torque developed from velocities is found.

Keywords: Wind turbine, Fluid Structure Interaction (FSI), CFD.

1. Introduction

Increasing demand of primary energy day by day in the world leads to set backs of rapid industrial development as well as shortages of the traditional energy resource. The emission of exhaust gas caused by excessive consumption of fossil fuels has also resulted in air pollution severely. Renewable energy, such as wind energy, solar energy, tidal energy and nuclear energy, has now been considered as an alternative resource to mitigate energy crisis. According to REN21's 2016 report in recent years, renewable energy contributed more than 20% to global energy consumption and electricity generation [1]. Wind energy is an abundant resource, particularly in Bangladesh, compared to other renewable resources. Wind turbine technology is also one of the cost-effective means for extracting energy from the wind. A wind turbine basically consists of rotors/blades mounted on a hub/shaft assembly, which transmits the produced mechanical power to the selected energy user. Although a significant amount of technological improvements had been done in relation to materials and cost to harness the wind effectively, the effect of wind on blade aerodynamic characteristics and their effects on blade structure have not fully investigated.

Early and continued research on wind turbines has made the field now more powerful as it employs advanced materials, electronics and aerodynamics [2]. Optimization tools are also used for improving performance and efficiency of wind turbines. The main focus of ongoing research is the design optimization of the wind turbine structures, realistic optimization models for enhancing blade aerodynamics and higher power output with minimum cost and weight. Studies report that the blade and the choice of airfoils are the most critical in designing a wind turbine. The lift generated from these airfoils at every section causes the rotation of the blade. Typically, nine airfoil families designed by National Renewable Energy Laboratory (NREL) and Airfoils, Inc. are used for various sized rotors [3]. In this study, the NREL S-series airfoil has also been used due to structural robustness from their thicker shape and largely insensitive to roughness. Propeller blades are another important parameter in wind turbine blade design. Blades are typically designed with a twist with higher angle at the hub than at the tip to balance the lift distribution along the blade.

A significant research had been done on the aerodynamic and structural modeling of wind turbines. Hsu and Bazilevs [4] presented the aerodynamics and fluid–structure interactions of the system and found that coupling FEM and IGA gives a good combination for efficiency, accuracy and flexibility of the computational procedure. Vasjaliya [5] defined a multidisciplinary design analysis optimization (MDAO) process for a composite wind

turbine blade to optimize its aerodynamic and structural performance by developing a fluid-structural interaction (FSI) system. Additionally, the evaluation of aerodynamic interaction of NREL Phase VI wind blade using FSI was studied by Lee et al. [6]. Although many other research had previously been conducted on wind turbine blade, but mostly for relatively higher twist angles (>20º). As such, in this paper a numerical study is performed for a low twist angled 9.5 meter long typical horizontal axis wind turbine (HAWT) blade. The investigation on the aerodynamic features of the wind turbine blade, the impact of different fluid flow conditions on the wind turbine blade and the structural strength is primarily focussed.

2. Methodology

2.1 Blade geometry selection

A number of blade models have first been tested with three different NREL airfoil families in various sections [7]. These three airfoils are, namely S818, S825 and S826, with S818 connects circular section in the blade rotor and the rest of the blade and S826 used at the tip. Total span of these modelled blades are within the range 9.5-41.25 m. However, only the blade of 9.5 m span is considered here due to minimize computational cost. The CAD view and the geometry of the wind turbine blade is shown Figure 1 and Table 1, respectively.

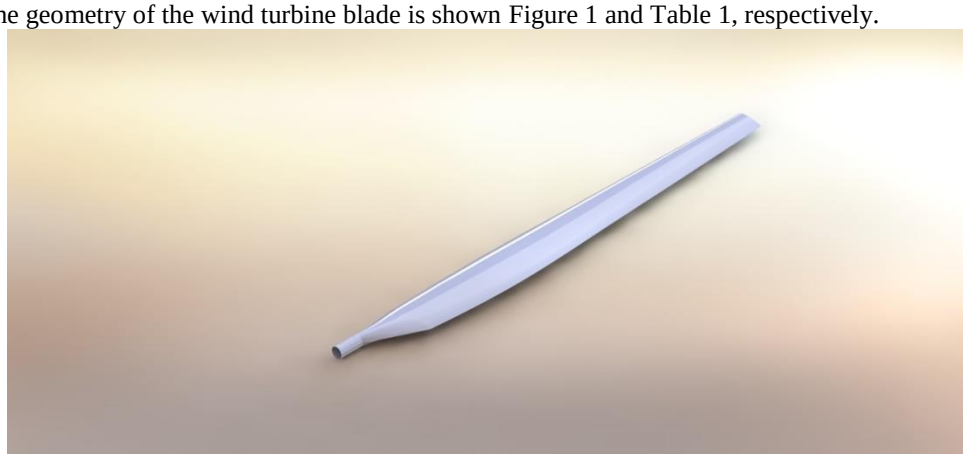

Figure 1. 3D CAD view of the wind turbine blade model (9.5 m span).

Table 1: The detailed geometry of the blade

Span(m)	Twist(degree)	Chord(m)	Airfoil
1	---	---	Circle
2	10	1.25	S818
4	7.5	1.5	
6	5	1.2	S825
8	2.5	0.75	
9.5	0	0.5	S826

2.2 Numerical analysis

In this study, Reynolds-averaged Navier-Stokes (RANS) approach has been used to simulate turbulent flows and the RANS equations is defined as:

$$\rho \frac{DU_i}{D_t} = \frac{\partial P}{\partial X_i} + \frac{\partial}{\partial X_i}\left[\mu \left(\frac{\partial U_i}{\partial X_j} + \frac{\partial U_j}{\partial X_i} \right) - \overline{\rho U_\iota U_J} \right. \qquad (1)$$

$\overline{\rho U_\iota U_J}$ is an unknown term and called Reynolds stresses [8]. The RANS equation is not closed due to the presence of stress term, so it requires a turbulence model to produce a closed system of solvable equation. In this regard, SST k-ω model is used to characterize turbulence. ANSYS 16.0 workbench simulation environment has been used to perform the FSI model. The blade geometry used has been primarily generated using Solidworks and then imported in ANSYS design modeler. Various body operations have been done on the blade and a fluid domain is created around it. That domain has been used for meshing and then the boundary conditions and initial parameters have been provided in mesh and setup section respectively. After obtaining the solution, the pressure distribution is imported in Static Structure to map that on the blade structure as load to determine the deformation and stress caused by that load.

The numerical domain consists of a far field region which is 5 meter upstream of turbine blade plane and 15 meter downstream. In this study, tetrahedral meshes have been chosen with variable sizing at different sections of the blade due to the complexity of model. Additionally, match control, face sizing, sphere of influence and inflation layer have been used in order to provide more uniform meshes. Such methods reduce to total mesh elements of 473k after grid independence tests. In contrast, in structural section, different types of mesh have been carried out for the blade, with a total element of 15k. Both fluid and structural meshes (enlarged view) for the blade only is shown in Figure 2.

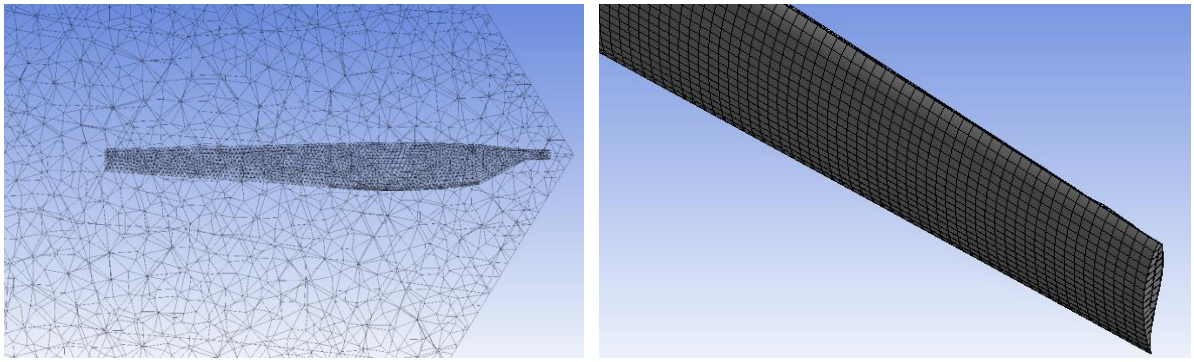

Figure 2. Meshes of the blade (zoomed in view): (left) CFD and (right) Structural

A second-order-upwind discretization technique and pressure based coupled solver has been used. Atmospheric air is used as fluid medium. Velocity inlet is chosen in the domain inlet with initial angular speed, and pressure outlet condition in the outlets. Also, periodic boundary condition is used for the interfaces. The convergence is assumed to achieve when the residuals of the variables reaches to 10^{-05}. For structural analysis, the boundaries and loads are defined in order to calculate the deflection and stress in the blade. The composite material properties for the blade have been taken from a standard GE 1.5 XLE wind turbine [9]. The significant feature in structural part is importing the effective forces from the ANSYS Fluent into the ANSYS mechanical. Therefore, the forces on each node in Fluent are effectively mapped into the mechanical node.

3. Results and discussion

Figure 3 represents the pressure contours at different planes at different velocities (4, 8 and12 m/s). The pressure difference between the suction and pressure side is found to be increasing with free stream velocity increment in the figure. Moreover, a more uniform static pressure is observed in the outer part of the blade (tip side) when velocity linearly increases.

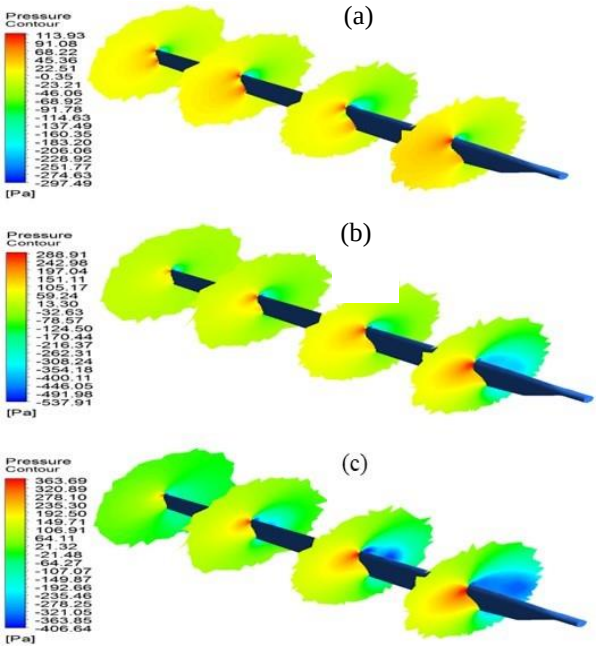

Figure 3. Pressure contours at different lengths of blade for (a) v=4 m/s, (b) v=8 m/s and (c) v=12 m/s

Figure 4 represents the 2-D cross sectional view of pressure contours and velocity streamlines respectively at different lengths, namely 25%, 50%, 75% and 95% from root to tip, for 8 m/s free stream velocity. Due to the larger negative pressure on the upper surface, lift force is generated and as a result the wind turbine blade rotates. The velocity of wind is higher at the upper surface and lower at the lower surface (Figure 5). This effect is opposite to those shown in Figure 3. Negative pressure can be explained by the wake generation from the blade. Again, flow separation occurs at the middle section near the root which gradually decreases. As free stream velocity further increases (not shown here), the pressure and velocity difference between upper and lower surface also increases causing higher lift. Larger flow separation occurs at leading edge with vortices along the span wise direction.

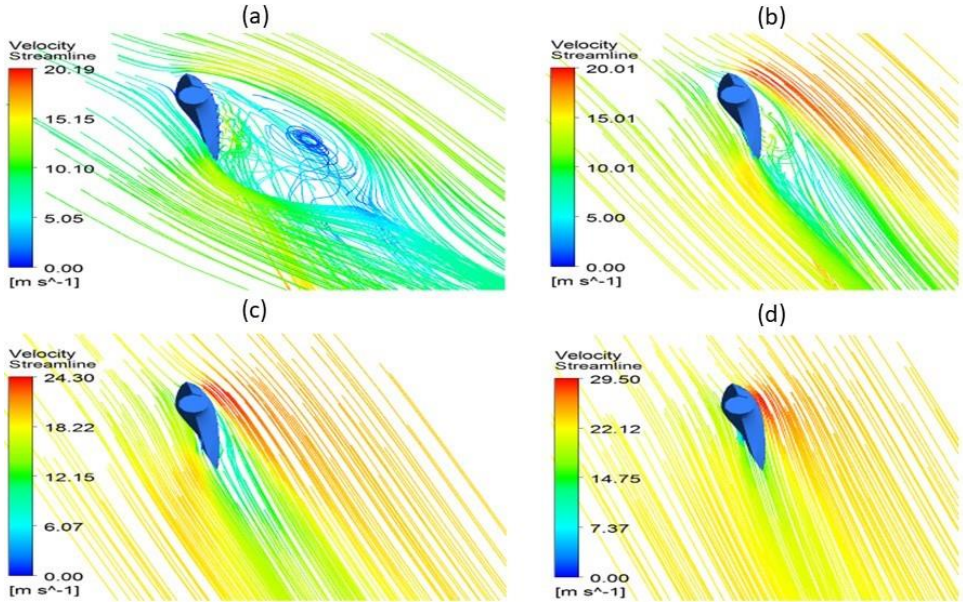

Figure 4. Velocity streamlines at (a) 25%, (b) 50%, (c) 75% and (d) 95% of span length for v =8 m/s.

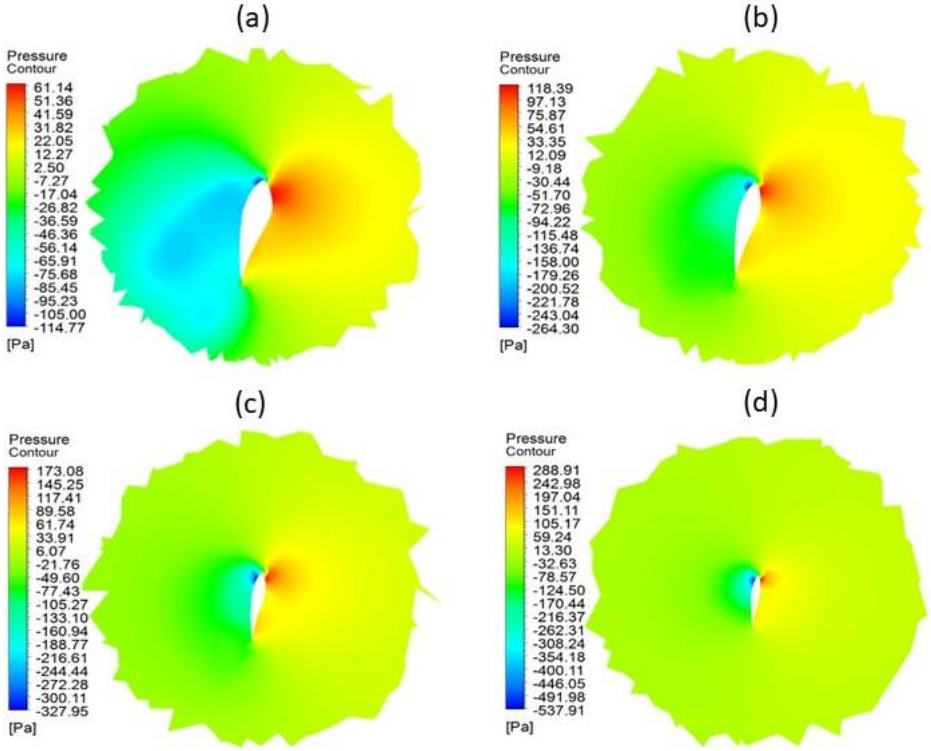

Figure 5. Velocity streamlines at (a) 25%, (b) 50%, (c) 75% and (d) 95% of span length for v =8 m/s

Figure 6 and Figure 7 show the deflection and equivalent stress on the blade at different velocities, respectively. The deflection occurs from about half of the blade length and largest deflect is near the blade tip. The magnitude of deflection is found to increase with the free stream velocity, but the overall behavior is insignificant for the range of velocity considered. Figure 7 shows the stress developed on the blade body against the forces acting on the blade. Despite the deflection occurs at the blade tip, interestingly the stress development appears to be concentrated near the root of the blade, where the blade may fail. Similar to the figure 7, the magnitude of stress increases with the increase of free stream velocity. For free stream velocity 4 m/s, 8 m/s and 12 m/s, maximum 0.04m, 0.05m and 0.07m deflections were found respectively. The stresses on the blade root for these velocities were 52 MPa, 73 MPa and 99 MPa respectively. It can be noted that the most deflection occurs at the 20%-30% span distance from the tip and most stress occurs near the root only.

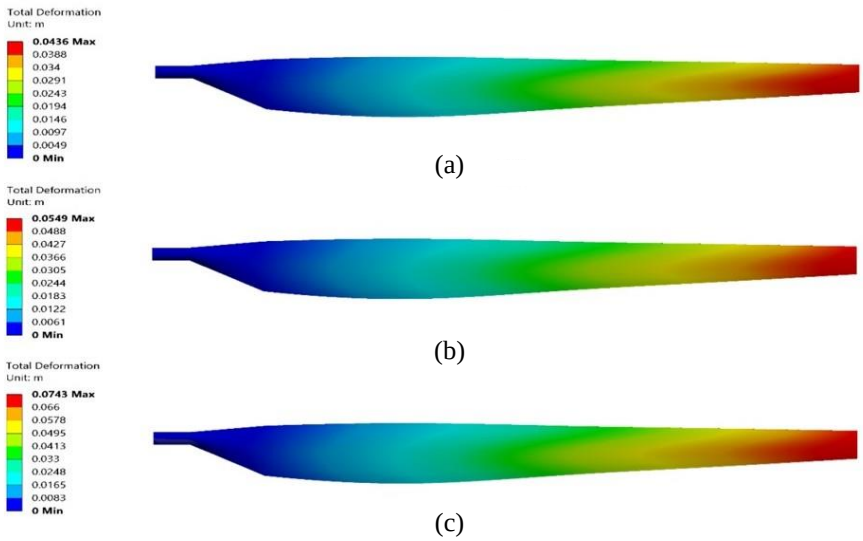

Figure 6. Deflection of blade for (a) v=4 m/s, (b) v=8 m/s and (c) v=12 m/s

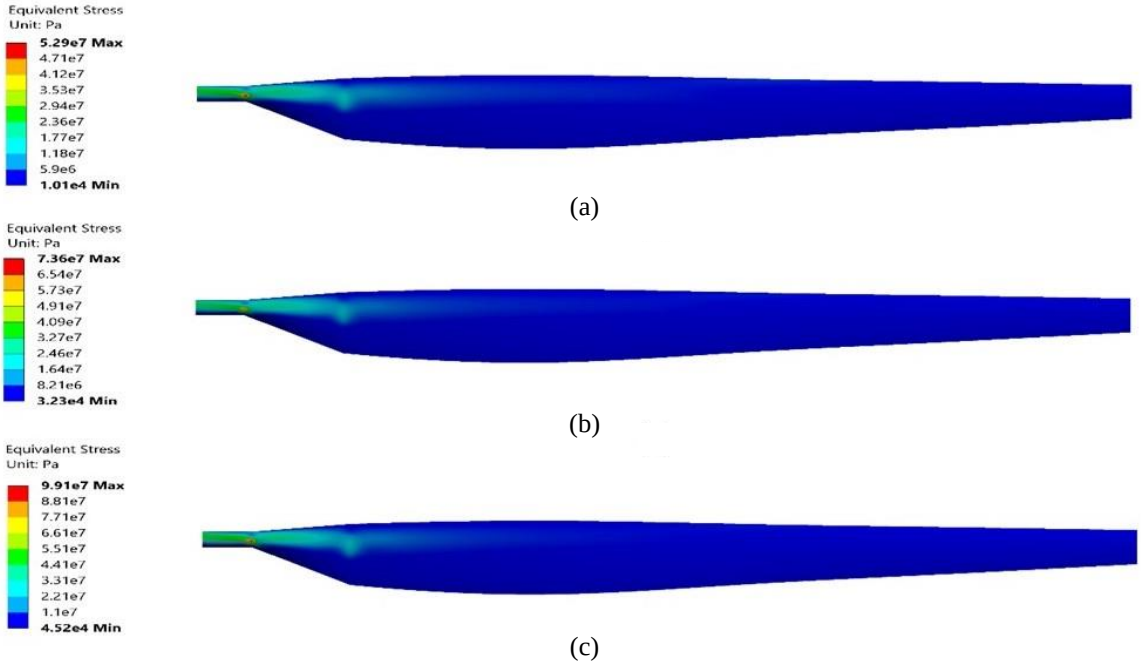

Figure 7. Stress of blade for (a) v=4 m/s, (b) v=8 m/s and (c) v=12 m/s.

Figure 8 presents the power curve for the selected wind turbine blade. The result indicates a moderately sharp increase in power with increasing free stream velocity. The power curve is then compared to that of a SERI-8 blade model [10]. Whilst the magnitude of power generation rate is different between these two blades, they show almost a predominantly similar behavior, i.e. a linear increase of power generation, except at the initial velocity.

The magnitude and slight deviation of the results are primarily due to the variation of blade geometry, such as length, angle of twist, airfoil shape, and angle of attack.

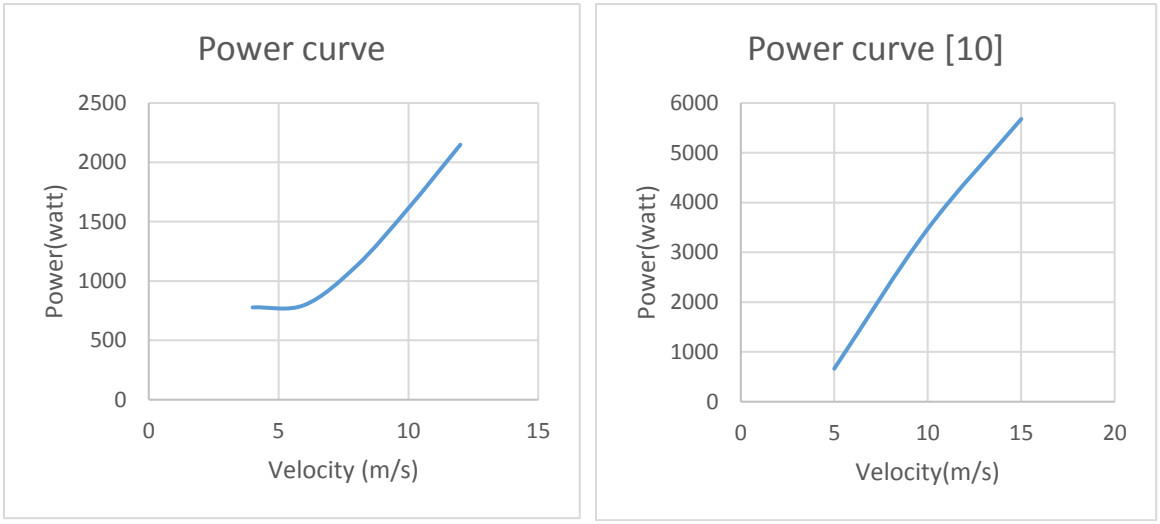

Figure 8. Power curves of the selected blade (left) and the SERI-8 blade (right) [10]

4. Conclusion

In this paper, the effect of free stream velocity on a wind turbine blade with low twist angle is investigated for aerodynamic behaviour and structural strength of the blade. In this regard, one-way FSI simulation was carried out on a typical wind turbine blade in ANSYS 16.0 for three different free stream velocities (4, 8 and 12 m/s). The calculated load in ANSYS Fluent was imported in ANSYS Static Structure as fatigue load and its' effect on the blade was analysed by the total deflection and equivalent stress on the blade. The pressure difference between the suction and pressure side increases with the increase of free stream velocity. Stronger flow recirculation occurs within the 50% of span, and the intensity is dependent of the free stream velocity. The starting position of the recirculation differs from other blade design due to the difference in twist angle. Most of the deflection occurred in the tip and most of the stress occurred in the root section whereas in other blades generally stress occurred in the middle portion. The blade was designed for moderate power generation and the power curve shows the linear increase in power for higher velocities. The power curve was plotted by the available torques at various velocities.

5. List of nomenclature

ρ	Air density
v	Free stream velocity
u	Flow speed of the object relative to the fluid
$\overline{\rho U_i U_j}$	Reynold's stress

6. References

[1] "Ran21 (Renewable Energy Policy Network for the 21st Century)'s 2016 report", 2016.

[2] Karam Maalawi, Special Issues on Design Optimization of Wind Turbine Structures, Wind Turbines, Dr. Ibrahim Al-Bahadly (Ed.), *InTech*, ISBN: 978-953-307-221-0, 2011.

[3] Tangler, J. L., and Somers, D. M., "NREL Airfoil Families for HAWTs", NRELfTP-442-7109, 1995.

[4] Ming-Chen Hsu and Yuri Bazilevs, "Fluid–structure interaction modeling of wind turbines: simulating the full machine", *Computational Mechanics*, Volume 50, Issue 6, pp 821–833, December 2012.

[5] Naishadh G. Vasjaliya, "Fluid-Structure Interaction and Multidisciplinary Design Analysis Optimization of Composite Wind Turbine Blade", Embry-Riddle Aeronautical University, 2013.

[6] Kyoungsoo Lee, Ziaul Huque, Raghava Kommalapati, and Sang-Eul Han, "The Evaluation of Aerodynamic Interaction of Wind Blade Using Fluid Structure Interaction Method", *Journal of Clean Energy Technologies*, Vol. 3, No. 4, July 2015.

[7] Calvin Phelps and John Singleton, "Wind Turbine Blade Design", Cornell University, Sibley School of Engineering, 2012.

[8] Deepak Sahini, "Wind Tunnel Blockage Corrections: A Computational Study", Texas Tech University, USA, 2004.

[9] Gagan Sahu and R.K. Rathore, "Determination of Torque Produced by Horizontal Axis Wind Turbine Blade Using FSI Analysis for Low Wind Speed Regime*", IJISET - International Journal of Innovative Science, Engineering & Technology,* Vol. 2, Issue 5, ISSN 2348 – 7968, 2015.

[10] Cheng-Huat Ong and Stephen W. Tsai, "The Use of Carbon Fibers in Wind Turbine Blade Design: a SERI-8 Blade Example", Department of Aeronautics& Astronautics, Stanford University, Stanford CA 94305-4035, 2000.